Journal of Applied Physics

Mitigating wakeup effect and improving endurance of ferroelectric HfO_2-ZrO_2 thin films by careful La-doping

Cite as: J. Appl. Phys. **125**, 034101 (2019); https://doi.org/10.1063/1.5050700
Submitted: 02 August 2018 . Accepted: 30 December 2018 . Published Online: 15 January 2019

Maxim G. Kozodaev, Anna G. Chernikova, Evgeny V. Korostylev, Min Hyuk Park, Roman R. Khakimov, Cheol S. Hwang, and Andrey M. Markeev

Journal of Applied Physics ARTICLE scitation.org/journal/jap

Mitigating wakeup effect and improving endurance of ferroelectric HfO_2-ZrO_2 thin films by careful La-doping

Cite as: J. Appl. Phys. **125**, 034101 (2019); doi: 10.1063/1.5050700
Submitted: 2 August 2018 · Accepted: 30 December 2018 ·
Published Online: 15 January 2019

View Online Export Citation CrossMark

Maxim G. Kozodaev,[1] Anna G. Chernikova,[1] Evgeny V. Korostylev,[1] Min Hyuk Park,[2] Roman R. Khakimov,[1] Cheol S. Hwang,[3] and Andrey M. Markeev[1,a)]

AFFILIATIONS

[1]Moscow Institute of Physics and Technology, Institutskii per. 9, 141701 Dolgoprudny, Moscow Region, Russia
[2]School of Materials Science and Engineering, College of Engineering, Pusan National University, 2, Busandaehak-ro 63beon-gil, Geumjeong-gu, Busan 46241, South Korea
[3]Department of Materials Science and Engineering and Inter-University Semiconductor Research Center, Seoul National University, Seoul 08826, South Korea

[a)]Author to whom correspondence should be addressed: markeev.am@mipt.ru

ABSTRACT

The crystalline structure and electrical response of La-doped HfO_2-ZrO_2 thin films of which processing temperature did not exceed 400 °C were examined, where the La-doping concentration was varied from zero to ≈2 mol. %. The film structure and associated properties were found to vary sensitively with the minute variation in the La-concentration, where the ferroelectric response at low La-concentration (<≈1 mol. %) gradually became antiferroelectric-like for La-concentration >≈1 mol. %, which was accompanied by a significant increase in dielectric permittivity. La-doping was found to be very effective in inhibiting the monoclinic phase formation and in decreasing the leakage current. Notably, the high coercive field, which was one of the most significant problems in this material system, could be decreased by ~35% at the most promising La-concentration of 0.7 mol. %. As a result, a highly promising field cycling endurance up to 10^{11} cycles could be secured while maintaining a high remnant polarization value (≥25 $\mu C/cm^2$). This is one of the best results in this field of the authors' knowledge.

INTRODUCTION

Doped-HfO_2-based ferroelectric (FE) thin films have already proved themselves as promising materials for ferroelectric memory technologies including ferroelectric random access memory (FRAM),[1] ferroelectric field-effect transistors (FeFETs),[2] and ferroelectric tunnel junctions (FTJs).[3,4] These materials provide the superior properties over traditional ferroelectrics with the perovskite structure such as scalability, including the possibility to grow these materials by atomic layer deposition (ALD), full complementary metal-oxide-semiconductor (CMOS)-compatibility even with the simpler crystal structure compared with the conventional perovskites. Under the term "HfO_2-based ferroelectrics," two groups of materials are usually consolidated. The first one is hafnium oxide doped by various elements (Si, Al, Y, La, Gd, etc.)[5–11] with relatively low concentrations, and the second one is a HfO_2-ZrO_2 solid solution (HZO).[12–15] Being the root cause of the FE performance in both groups, the orthorhombic phase (space group $Pca2_1$, o-phase) seems to always coexist with other polymorphs of HfO_2, such as monoclinic (space group $P2_1/c$, m-phase), tetragonal (space group $P4_2/nmc$, t-phase), or even cubic (space group $Fm3m$, c-phase). This is not an optimal aspect of this ferroelectric material system. It is worth noticing that the absence of the most stable (for the bulk material) m-phase is perceived as an indication of the preferred formation of metastable phases including the FE o-phase.

Among them, HZO solid solution attracts a great deal of attention due to its lower crystallization temperature (≈400 °C)

compared with other doped-HfO_2 films or even undoped HfO_2.[12–15,16] This low processing temperature meets the back-end-of-line (BEOL) limitations, making it well suitable for FRAM production in the one transistor-one capacitor structure. However, HZO usually includes a significant portion of the m-phase, depending on its precise composition and annealing conditions, which deteriorates the remnant polarization (P_r) value.[13] It is also worth noting that phase transitions in these films are also strongly influenced by the substrate properties. Several recent studies revealed a correlation between structural properties and FE response of HZO films grown on Pt and Ir films.[17,18] In particular, the bottom electrode material could significantly change the average grain size, which is a key enabler of phase transitions. A significant difference between m-phase fractions was demonstrated for HZO films with different compositions, grown directly on Al_2O_3-passivated Si or Ge substrates, studied by grazing incidence synchrotron irradiation.[19] However, in that work, a specific crystallization process was repeatedly performed at 800 °C after each 20 ALD cycles [deposition-annealing (DADA) sequence]. The preferential growth of the tetragonal HZO phase following bottom-up crystallization during the DADA ALD process was also demonstrated.

In contrast, doped-HfO_2 films have provided the possibility to inhibit m-phase formation considerably or even completely but usually at the cost of the increase of the thermal budget. Among the doping elements, ones with large atomic radii, including La or Gd, were demonstrated to have the strongest effect on the stabilization of the FE o-phase both experimentally and computationally.[1,8,20] Among the various dopants, La with a relatively low concentration (~1 mol. %) demonstrated the possibility to improve the FE performance without a significant increase in the thermal budget.[21] However, such a low doping level resulted in the incomplete m-phase suppression, which could have partly deteriorated the FE performance. Consequently, there always seems to be a trade-off between the appropriate crystalline structure and the thermal budget of the formed HfO_2-based ferroelectrics.

For the device performance side of the HfO_2-based ferroelectrics, a field cycling endurance, which is extremely important for working memory applications, is still a serious problem. All the reported HfO_2-based FE films possess a high coercive field E_c (typically, ≥1.0 MV/cm), which requires high driving voltage (≥3.0 V for 10 nm-thick films) to reach the saturated remnant polarization ($2P_r$) value, and thus, degrades their reliability. According to the current understanding, the general failure mechanism of these films is a hard breakdown, which is generally related to the accumulation of oxygen vacancies.[22] The crystallization with a low thermal budget, therefore, might be an efficient method to decrease oxygen vacancy concentration, which will increase the number of field switching cycles to the breakdown. This is especially the case because the most commonly adopted electrode material is titanium nitride (TiN), which can induce the oxygen vacancy formation in the HfO_2-based layers by the chemical reaction during the film growth or post-deposition annealing (PDA). Therefore, it is an impending task to decrease the E_c, while maintaining the low thermal budget to improve the field-cycling reliability. Due to the involvement of the early breakdown in these materials, the genuine fatigue, which means the decrease in P_r with the increasing switching cycles, has been barely observed. Fatigue performance is another critical measure for the material performance to the memory device application.

Recently, the authors demonstrated that the formation of the more complex multi-component system, namely, La-doped HfO_2-ZrO_2 (HZLO), could be the viable solution to the above-mentioned problems.[23] No m-phase formation after rapid thermal processing (RTP) at temperatures as low as 450 °C and 500 °C was observed. Besides, HZLO demonstrated the considerable decrease in the E_c and direct current (DC) leakages compared to HZO, which led to the enhancement of the field cycling endurance up to 4×10^{10} cycles. Nonetheless, comprehensive insights that would exploit the full potential of this system are still missing. Therefore, in this work, the structural and electrical properties of HZLO within a very narrow range of La-concentration range were carefully examined after "*in situ*" (or "automatic") crystallization during top TiN electrode deposition at 400 °C to expand the current knowledge of this complex system and reveal its full potential. In addition, the influence of the RTP at elevated temperatures is also discussed.

Previously, it was also shown that HZLO could demonstrate the stable antiferroelectric (AFE)-like behavior after the RTP at 400 °C.[23] Such a phenomenon opens up the alternative opportunity of using this material for the highly efficient electrostatic supercapacitors, which was already demonstrated by the examples of HfO_2-ZrO_2,[24] Si-doped HfO_2,[25] and even multi-component systems such as Al-doped HfO_2-ZrO_2 or Si-doped HfO_2-ZrO_2.[26] However, the desired AFE-like behavior was achieved only after 500 °C annealing. Therefore, current work is also aimed to examine the possibility of the stable AFE-like response in HZLO films, obtained by BEOL-compatible processes.

EXPERIMENTAL PROCEDURE

TiN/HZLO/TiN capacitor structures were formed on 3 in. silicon wafers with 100 nm-thick plasma-enhanced chemical vapor deposited SiO_2 and 50 nm-thick sputtered W layer for electrical insulation and decreasing the contact resistance, respectively. Both top and bottom TiN electrodes (20 nm-thick) were grown by a conventional thermal ALD method at a substrate temperature of 400 °C using $TiCl_4$ and NH_3 as the Ti-precursor and nitrogen source, respectively. This thermal ALD process was utilized instead of the plasma-assisted ALD (PAALD),[27] which was performed at 320 °C in the previous work,[23] in order to verify the possibility of the "*in situ*" crystallization of the underlying HZLO layer during top electrode deposition. The total top TiN deposition time was ≈4 h, after which samples were immediately unloaded to the load-lock system. This could be an effective approach for the implementation of such FE capacitors to a BEOL process, avoiding the PDA. Tetrakis(ethylmethylamino)hafnium (TEMAH), tetrakis(ethylmethylamino)zirconium (TEMAZ), tris(isopropyl-cyclopentadienyl)

lanthanum [La(iPrCp)$_3$], and O_2-plasma were used as the Hf, Zr, La-precursors, and oxygen source, respectively, to grow the 10-nm-thick HZLO films at a substrate temperature of 235 °C. The La/(Hf + Zr) ALD cycle ratio was varied from 1/32 to 1/7 to achieve the different La-concentrations (from ≈0.4 to ≈2.0 mol. %, respectively). Five different films with 0.4, 0.7, 1.0, 1.4, and 2.0 mol. % La-concentrations were grown. In addition, a similar HZO-based capacitor structure was also formed as a reference for subsequent experiments. The details for calculation of the La-concentration are presented in the supplementary material. The estimated La content, as well as the Hf/Zr ratio, was confirmed by X-ray photoelectron spectroscopy (XPS) measurements (Figs. S1–S3 in the supplementary material).

RTP in the N_2 environment for 30 s at temperatures (T_{ann}) of 500 °C and 600 °C was applied after the top TiN deposition selectively to some samples, which was performed to examine the PDA effect separately.

The structural properties of the as-grown (after the "automatic" crystallization) HZLO films and the reference HZO were examined by grazing-incidence X-ray diffraction (GIXRD) with Cu Kα radiation using an incident angle of 1°. The spectra were collected with a 0.02° step resolution and integration time as 70 s, with the presence of the 20-nm-thick top TiN layer.

The surface morphologies of the as-grown films were studied by scanning electron microscopy (SEM). For this purpose, the top TiN electrode was removed in advance by dipping the sample into H_2O_2 (37%) solution for 15 min at 50 °C. The grain size distributions were extracted from the obtained SEM images by the watershed method implemented by the Gwyddion software.[28]

For electrical measurements, top contact pads with an area of $\approx 2 \times 10^{-5}$ cm^2 were formed in the top TiN electrode by a lithographic process followed by a plasma-etching in SF_6. Small-signal capacitance-voltage (C-V) measurements with an AC signal frequency of 10 kHz and amplitude of 50 mV were used to estimate the dielectric constant (k). Dynamic hysteresis currents were measured in response to the triangular voltage sweeps with 0.4 kHz frequency, while P-E hysteresis loops reconstruction was derived by their integration. Endurance measurements were performed by the positive-up-negative-down (PUND) technique using bipolar cycles with different voltage pulse amplitudes and a constant pulse duration of 0.6 μs (0.2 μs rise and 0.2 μs fall times, respectively).

RESULTS AND DISCUSSION

As it was emphasized above, the as-deposited HZLO films were subjected to only "automatic" annealing at a temperature of 400 °C to induce the crystallization, so it was of particular interest to see if the crystallization actually occurred. The as-deposited films were almost completely amorphous (data not shown). The GIXRD spectra collected from HZO/HZLO films are presented in Fig. 1(a). According to the previous experimental works, the most interesting 2θ range is 27°–38° since it contains the most intensive peaks of the HfO_2-based films, which permitted accurate structural analysis. The presented spectra consist of two sharp peaks from HZO/HZLO, as well as a peak located at 2θ ≈ 36.9°, which is attributed to the cubic TiN. As it was expected from the previous results,[23] the La-doping showed a high efficiency to the m-phase suppression; the peaks at 2θ ≈ 28.5° and ≈31.6°, corresponding to the most intensive (–111) and (111) m-phase reflections, can be clearly seen in the case of HZO, but they completely disappeared during the La-addition (at 0.7 mol. % or higher). It is worth noting that the disappearance of the monoclinic (111) and (–111) diffraction peak cannot completely prove the absence of the monoclinic phase in the doped HZO thin films in principle. For the case when the film texture is strongly affected by doping concentration, the two main diffraction peaks from the monoclinic phase disappear, but the other diffraction peaks from monoclinic phase can be still observed. Nonetheless, it is reasonable to assume that the La-doping might not significantly change the texture of the La:HZO thin films since diffraction peaks which correspond to other phases do not vanish. Moreover, the electrical measurements also support a significant decrease in the monoclinic phase fraction with the disappearance of the monoclinic (111) and (–111) diffraction peaks. Simultaneously, two diffraction peaks at 2θ ≈ 30° and ≈35°, usually attributed to the combination of o/t phases [(111) and (002) reflections, respectively], and, probably, a small contribution from the c-phase also, may give important information about the film structural changes.

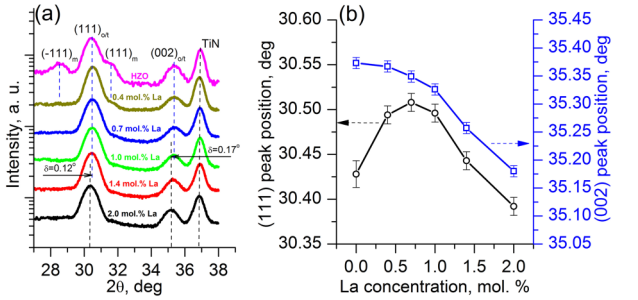

FIG. 1. (a) GIXRD collected from HZLO with different La-concentrations and HZO-based capacitors after "automatic" annealing; (b) related (111) and (002) peak positions as a function of the La concentration in HZLO films.

The $(111)_{o/t}$ and $(002)_{o/t}$ peak positions (2θ values) extracted from Fig. 1(a) are presented as a function of the La-concentration in Fig. 1(b). It should be noted that a double-sized unit cell with four Hf^{4+} and eight O^{2-} ions was considered for the t-phase for the sake of convenience. The $(111)_{o/t}$ peak position showed an increasing tendency up to 0.7 mol. % La and decreased upon further La-concentration increase, while the $(002)_{o/t}$ peak monotonically decreased from 35.37° to 35.18° with an increase of the La-concentration. Here, it should be noted that the diffraction peaks in Fig. 1(a) are quite broad due to the nanoscale size of crystallites. As a result,

some diffraction peaks can be attributed to the overlap of several diffraction peaks from different crystalline phases. Dey *et al.* reported that the diffraction peak at ~35° obtained from $Hf_{1-x}Zr_xO_2$ thin films can be an overlap of diffraction peaks from the strained tetragonal phase and various orthorhombic phases.[19,29] However, due to the reason above, o- and t-phases cannot be completely separated even with the X-ray from the high-energy synchrotron source.

In general, peak shift may be caused by two reasons with different nature. The first one is a mechanical stress and the second reason is the change in relative fractions of different crystalline phases such as t- and o-phases, both of which depend on the doping level. In order to gain deeper insights into the reasons for the observed peak shift, the method proposed by Park *et al.*, who focused on the so-called relative ratio (R_a, or the tetragonality value) of different phases was adopted.[30,31] It was reported that R_a, which is determined as a relative ratio of the longer axis to the shorter axis [c/a for the t-phase and $2a/(b+c)$ for the o-phase], is significantly different for o- and t-phases.[31] It should be noted that the longest axis is theoretically a and c for o-phase and t-phase, respectively. Therefore, a and c lattice parameters were extracted from the measured peak positions [Fig. S5(a) in the supplementary material]. In these calculations, no difference between b and c lattice parameters in the o-phase was assumed (it was reported that difference is less than 0.4% even in a bulk phase[31]). The calculations revealed that the theoretically longest axis (c for the t-phase or a for the o-phase) decreased from ≈5.12 Å down to ≈5.07 Å for the doping level of 0.7 mol. % La and then slightly increases to ≈5.08 Å at higher La-concentration. At the same time, the theoretically shortest axis monotonically increases from ≈5.07 Å to ≈5.10 Å with the La-concentration increase from 0 to 2.0 mol. %. Interestingly, the theoretically shortest and the longest axis become equal ($R_a = 1$) at La-concentration of 0.7 mol. %. Meanwhile, R_a monotonically decreases from ≈1.01 to ≈1.00 [Fig. S5(b) in the supplementary material] with the increasing La-concentration in this work, which is consistent with previously reported results.[31] It is believed that the films in this work have the o- (low La-concentration region) or t-phase (high La-concentration region) structure with a lattice constant very similar to the cubic phase whose R_a is 1. In addition, the investigated films may be under quite high tensile biaxial stress, which has been reported in similar films elsewhere. However, the adopted GIXRD geometry did not permit to estimate the out-of-plane direction strain in this work. Nonetheless, the lattice parameter variations according to the La-concentration indicated that 0.7 mol. % coincided with the point where the film structure underwent a structural phase transition (perhaps coincident to the morphotropic phase boundary), where the FE performance might be improved.[31] This was indeed the case as shown below.

It has been well reported that the phase evolutions in thin HZO films are largely influenced by the grain size and its distribution.[14] Therefore, the SEM images of the undoped HZO and 0.7 and 2.0 mol. % of La-doped HZLO were obtained [Figs. S4(a)–S4(c) in the supplementary material], and their grain size distributions are presented in Fig. 2.

As can be seen from this figure, the HZO film showed a peak distribution of the grain size at ≈6 nm of radius with a relatively symmetric distribution with respect to the peak grain size value. In contrast, the HZLO films showed the peak values at the grain diameter of ≈3-5 nm, with much more asymmetric distribution. It can be noted that the distribution has a broad peak near the radius of ≈8-10 nm, which is the main reason for the involvement of the asymmetry. There was no critical difference in the average grain size and its distributions between the two differently doped HZLO films. Therefore, the La-doping appears to mainly influence the grains with a smaller diameter in the HZO film and made them even smaller, while the larger grains less influenced. Such observation, however, is not consistent with the authors' previous report on that the La-addition resulted in the grain growth.[23] The reason for such discrepancy is most likely ascribed to the imperfectness of the HZO film in the previous work, which involved a high leakage current. Also, the different crystallization processes (automatic in this work vs. RTA in the previous work) may have contributed to the difference, but further research is necessary to elucidate the reasons clearly. Next, the electrical properties of the HZLO films according to the La-concentration were examined.

Figures 3(a)–3(l) show k-E curves derived from the small signal C-V measurements, and P-E curves of HZO and different HZLO-based capacitors, respectively. These curves were measured both in "pristine" and in "awakened" (10^5 cycles of bipolar rectangular pulses with 3.0 MV/cm amplitude and 30 μs duration) states (black and red curves, respectively). This is important because the multiple switching may result in significant structural/chemical changes, and consequent electrical modifications due to the so-called wake-up effect.

It can be clearly seen that the k-E curves at the pristine state (black lines) qualitatively reproduce the FE behaviors at least for the HZO film and HZLO films with 0.4 mol. % and 0.7 mol. % La, where the obvious peaks in the positive and negative voltage region correspond to E_c and $-E_c$. However,

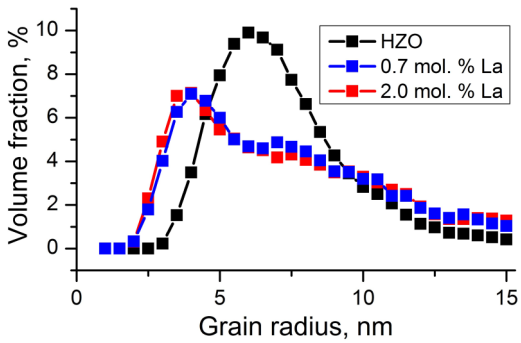

FIG. 2. The extracted grain size distributions from SEM images for 0.7 and 2.0 mol. % La-doped HZLO and HZO films. Lines serve as a guide for the eye.

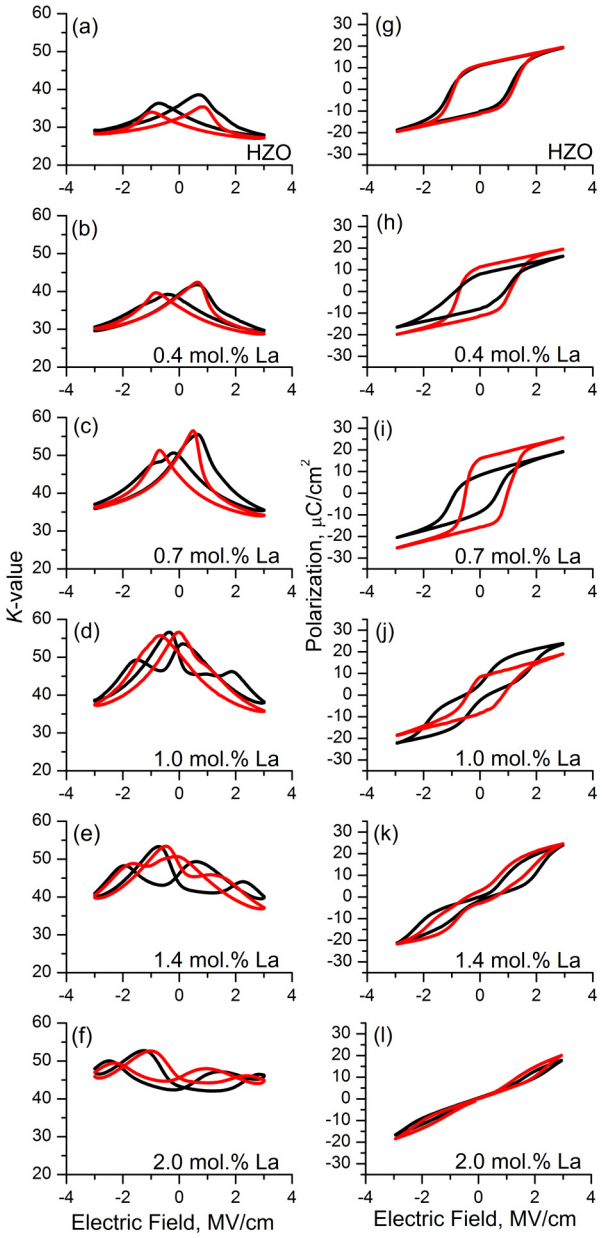

FIG. 3. *k*-E curves derived from the small-signal C-V measurements of HZO (a) and HZLO-based stacks with different La-concentrations (b)–(f); related P-E hysteresid curves (g)–(l). Black curves correspond to the "pristine" state (no electrical impact was applied prior to the measurement), whereas red curves correspond to the measurements carried out after wake-up cycling with bipolar voltage pulses (10^5 cycles with 3.0 MV/cm amplitude and 30 μs duration).

the curves involved humps and subsidiary peaks, especially during the sweep from the positive to the negative direction, suggesting the non-uniform ferroelectric properties across the electrode area. This can be attributed to the non-uniform involvement of defects, which may hinder the domain motion and non-uniform grain size distribution shown in Fig. 2. However, they disappeared after the wake-up procedure [red line in Figs. 3(a)–3(c)], suggesting the depinning of the domains. A clear FE behavior for the cases of the two low La-concentrations was also confirmed by P-E hysteresis measurements even for the pristine films [black curves in Figs. 3(g)–3(i)]. The wake-up results in an obvious increase in the $2P_r$ from $\approx 16\,\mu C/cm^2$ to $\approx 22\,\mu C/cm^2$ and from $\approx 18\,\mu C/cm^2$ to $\approx 31\,\mu C/cm^2$ for films with 0.4 mol. % and 0.7 mol. % of La-concentration, respectively, whereas the HZO film showed relatively wake-up free behavior. This will be discussed in more detail later.

Both *k*-E and pinched P-E curves obtained from the sample with 1.0 mol. % of La at the pristine state indicated a partial AFE-like behavior. In our previous work, where HZLO with a similar composition was analyzed,[23] the RTP at 400 °C resulted in a pronounced and quite stable AFE-like behavior. It has been known, however, that HfO_2-based ferroelectrics are quite sensitive not only to precise composition but also to the annealing conditions.[13] In the current work, the rather long "*in situ*" annealing was applied instead of RTP. The partial crystallization of HZLO films could take place during top electrode deposition at 320 °C before the subsequent RTP in the previous work.[23] Consequently, the behavior of HZLO (1.0 mol. %) film significantly differs from the previous result. It can be seen from Fig. 3(j) that wake-up cycling resulted in the completely depinched P-E hysteresis. Accordingly, the related *k*-E curve took the FE-like shape as well, while $2P_r$ increased from $7\,\mu C/cm^2$ to $16\,\mu C/cm^2$.

Qualitatively the same but less pronounced transformation from mostly AFE-like to a partial FE behavior with final $2P_r$ as low as $\approx 5\,\mu C/cm^2$ as a result of wake-up was observed from the films with the further increased La-concentration up to 1.4 mol. %. However, the HZLO film with 2.0 mol. % of La showed quite stable AFE-like behavior before and after the wake-up.

The extracted $2P_r$ (in the awakened state) and *k* values taken at 3.0 MV/cm for all films are summarized in Fig. 4(a). It can be understood that the observed continuous change from mostly FE to the mostly AFE-like behavior is accompanied by the rise of *k* from ≈29 to ≈45 along with the increasing La-concentration. The highest-*k* phase both for HfO_2 and HZO polymorphs is known to be the t-phase.[13] Therefore, it could be inferred that t-phase formation becomes more preferred with an increase of La-concentration compared to the o-phase, of which variation could be confirmed by the FE to AFE transition. The AFE-like response could be explained by the reversible t ↔ o field-induced phase transition, which was suggested for other HfO_2-based AFE films.[32] As mentioned above, such behavior is of interest for energy-storage applications; therefore, the detailed investigations of this film were also carried out.[33] The far lower *k* values of ≈29 and ≈30 in cases of HZO and HZLO with the 0.4 mol. % La-concentration seemed to indicate the possible involvement of the m-phase ($k \sim 17$) in these films, which can also be confirmed from GIXRD in Fig. 1(a).[13]

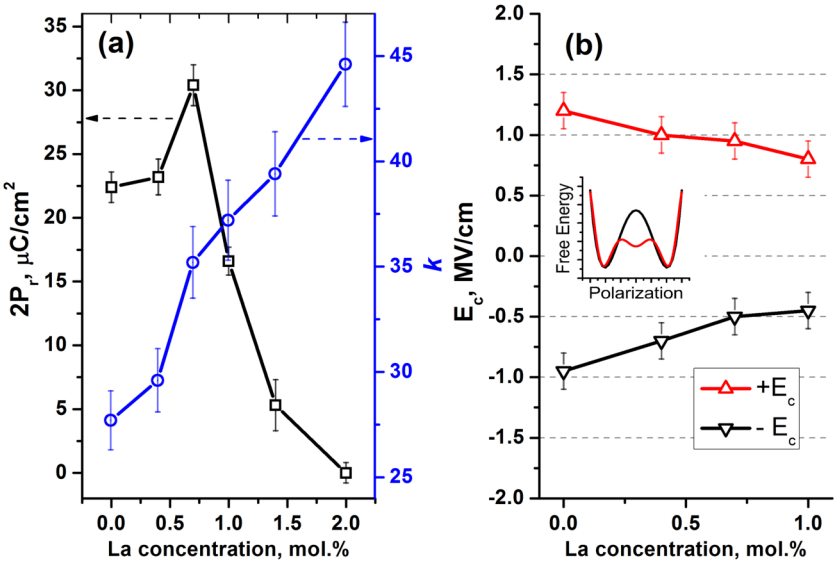

FIG. 4. (a) Influence of La-concentration on the dielectric permittivity k and $2P_r$ value; (b) evolution of negative ($-E_c$) and positive ($+E_c$) coercive fields with the increase of La-concentration in stacks, where FE response was observed after 10^5 wake-up cycles. Inset: The free energy-polarization curve of a ferroelectric film with (red curve) or without (black curve) the involvement of the non-polar t-phase.

Now, it becomes evident that HZLO behavior is very sensitive to its minute change in La-concentration in this narrow range. According to Fig. 4(a), only the HZLO film with 0.7 mol. % of La showed significantly higher $2P_r$ that of HZO after the wake-up process, whereas they showed similar $2P_r$ values at pristine states. However, there is another critical feature, which favorably distinguishes the HZLO system from HZO and most other HfO_2-based ferroelectrics, as shown in Fig. 4(b), which shows the variations in the $+E_c$ and $-E_c$ values as a function of La-concentration up to 1 mol. % (richer La films were mostly AFE so E_c's can hardly to be defined). There is almost a 35% decrease in both E_c values when the La-concentration was ~1 mol. %, suggesting that the field-cycling to test the endurance and eventual fatigue (by the domain pinning[34]) could be performed at a lower field.

The possible reason for decreasing E_c can be suggested from the increasing stability of the t-phase with the increasing La-concentration. Since the t-phase has the lowest energy near P = 0 state, whereas the o-phase has its lowest energy at $+P_r$ and $-P_r$ states, according to the Landau formalism, there can be a local minimum near the origin of the free energy-polarization curve (U–P) as schematically shown in the inset figure of Fig. 4(b) (red curve).[35,36] The involvement of such a local minimum can decrease the energy barrier between the $+P_r$ and $-P_r$ states compared with the pure o-phase [of which the schematic U-P diagram is also included in the inset of Fig. 4(b) (black curve), where there is no local energy minimum near the origin], which could decrease the E_c values. The presented considerations are consistent with the structural changes discussed earlier, since the unit cell volume decreases from ≈131.6 (mostly the o-phase) down to ≈130.6 Å^3 (combination of t- and o-phases) with the increase in the La-concentration up to ≈1 mol. % (Fig. S6 in the supplementary material). It should be noted that the polarization switching process of the HZLO film should be dominated by nucleation and growth of oppositely polarized domains. Thus, the aforementioned Landau model is not an only factor which determines the E_c value of the HZLO film. However, the nucleation of oppositely polarized domains should be affected by the energy barrier in the inset of Fig. 4.

In order to verify the positive effect of La-doping in detail, the cycling endurance tests of HZO and HZLO films were performed with the different field amplitudes: 3.5, 3.0, and 2.5 MV/cm, and the results are presented in Fig. 5. The HZLO film with the highest La-concentration was excluded because it showed the stable AFE-like responses. For the case of 2.5 MV/cm, only results obtained from the two HZLO films with the lowest La-concentrations are presented because the above-mentioned AFE to FE transition during field cycling was not notable in these cases.

At the highest field strength of 3.5 MV/cm, all the films suffered from the early breakdown at ~10^9 cycles, except for the 1.4 mol. % La-concentration film. However, this film showed a significant wake-up behavior, and a low $2P_r$ value (≈9 μC/cm^2) even after the complete wake-up. Therefore, this film could not be a feasible material for the memory applications. Nonetheless, the HZLO film with 0.7 mol. % La showed the highest $2P_r$ value of ≈37 μC/cm^2 just prior to the breakdown, demonstrating its great potential. A similar trend could be observed when the cycling field was

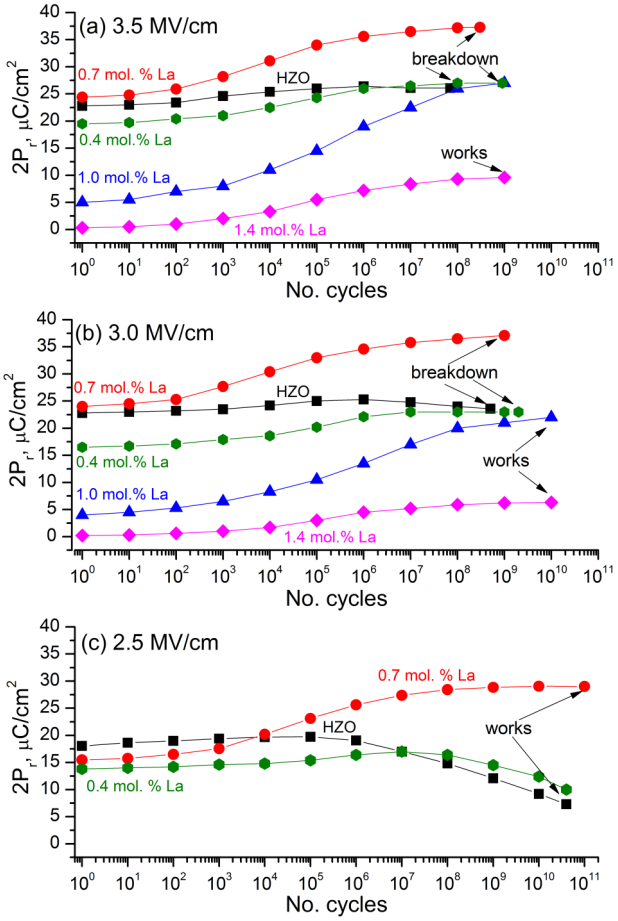

FIG. 5. Endurance characteristics measured by PUND from HZO and HZLO-based stacks with different La-concentrations. During PUND measurements pulse duration remained constant (0.6 μs), while the pulse amplitude varied: (a) 3.5 MV/cm, (b) 3.0 MV/cm, and (c) 2.5 MV/cm.

decreased to 3.0 MV/cm with an improvement of the endurance cycle by one order of magnitude for the films with higher La-concentrations, but the similar endurance cycles at lower La-concentrations. The maximum achievable $2P_r$ values were not significantly deteriorated by the decreased cycle field strength.

When the cycle field was decreased to 2.5 MV/cm, the HZLO film with optimum La-concentration (0.7 mol. %) demonstrated a highly promising performance up to 10^{11} cycles without the breakdown or fatigue, while a reasonably high $2P_r$ value of $\approx 28\,\mu C/cm^2$. In contrast, the HZO film showed a significant fatigue, i.e., the $2P_r$ value was decreased from $\approx 18\,\mu C/cm^2$ to $\approx 9\,\mu C/cm^2$ only after the 10^{10} cycles albeit it was not permanently broken down. The 0.4 mol. % La-doped HZLO film showed an intermediate performance without the breakdown at 10^{10} cycles under the same conditions. Another notable point is the wake-up degree which could be estimated as a ratio of $2P_r$ in saturated (e.g., after 10^8 cycles) and pristine states. For the case of the film with 0.7 mol. % La, this ratio is $\approx$1.80 and 1.50 for 2.5 MV/cm and 3.5 MV/cm, respectively. Being compared with the previous result,[23] where the ratio was as high as $\approx$3.8, the $2P_r$ stability was significantly improved too in this sample, which might be ascribed to the different crystallization process (*in situ* automatic vs. RTP).

The breakdown and fatigue in FE films are closely related with the leakage current, because the leakage current induces a cumulative Joule heating and charge trapping effects during the repeated endurance cycles.[37,38] Therefore, it can be anticipated that the better performance of the optimum La-concentration film against the breakdown and fatigue might be induced from the decreased leakage current, which could be indeed confirmed by Fig. 6(a). It can be understood that the leakage current was largely decreased by the increasing La-concentration in the pristine state. For all the films, the leakage current was increased after the 10^7 cycles at 2.0 MV/cm, but the degree of increase decreased with the increasing La-concentration. However, there is a large deterioration in the FE performance for the films with La-concentration $>\approx$1.0 mol. %. Therefore, the HZLO film with La-concentration of 0.7 mol. % appeared to be the optimum one considering the low leakage current (high reliability) and high $2P_r$ (high performance).

To further supplement this conclusion, the additional RTP was performed for the 0.7 mol. % HZLO film. Figure 6(b) demonstrates that the RTP incurs a significant rise of the leakages both at the pristine state and after 10^7 times of switching cycles, which induced the significant decay in the reliability as shown in Fig. 7.

Figure 7 depicts the adverse influence of RTP to the endurance performance tested at 2.5 MV/cm. Firstly, it is worth noting that the ratio between the remnant polarization in the fully saturated state (e.g., after 10^8 cycles) and pristine state monotonically decreases with the annealing temperature increase (from 1.87 after "automatic annealing" down to 1.42 after 600 °C RTP). Nevertheless, despite the observed possibility to increase the $2P_r$ value by RTP (for 550-600 °C) at the pristine state, it is evident that even 500 °C annealing leads to the speed-up of the hard breakdown. Thus, the switching was limited to $\approx 4 \times 10^9$ cycles for any RTP, whereas "no RTP" sample was still working even after the 10^{11} cycles. Thus, the advantage of "*in situ*" annealing at relatively low-temperature annealing over RTP for the lower leakages and higher reliability of HZLO-based stacks can be confirmed.

Finally, the reason why *in situ* crystallization at 400 °C during TiN deposition can enhance the endurance of HZLO compared to the crystallization processes by the RTP at temperatures >500 °C. There exist two thermally activated processes in ferroelectric doped HfO_2 thin films: the formation of the FE o-phase and the formation of oxygen vacancies. The kinetics of the two mechanisms needs to be carefully examined to understand the endurance improvement of the HZLO system. Mueller *et al.* reported that during the

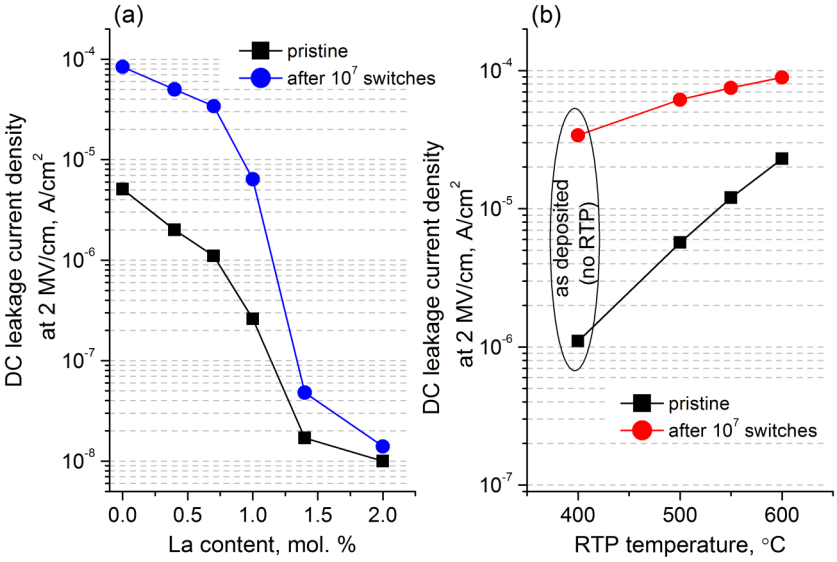

FIG. 6. (a) Leakage current densities at 2 MV/cm in dependence of La-concentration, measured at pristine state and after 10^7 switching cycles and (b) 2.0 MV/cm leakage current density evolution of 0.7 mol. % of La-based stack with an increase of RTA temperature, measured at pristine state and after 10^7 switching cycles.

crystallization process of HZO thin films, the amorphous films are crystallized first into the t-phase, and it finally changes to the FE o-phase.[12] Park *et al. in situ* observed a two-step crystallization process from amorphous to the o-phase via the t-phase in the HfO_2 thin films doped with Si, Al, Gd, and Sr[39] using an *in situ* X-ray diffraction with increasing temperature. They also showed that it is the reason why the P_r value increases with increasing annealing temperature in the doped HfO_2 films.[39] The kinetic energy barrier between the t-phase and the o-phase was calculated using computational simulation[40–42] and was also experimentally estimated by several research groups.[43,44] From both theory and experiment, the estimated kinetic energy barrier was as low as 0.03-0.05 eV/f.u., which might originate from the martensitic phase transition with sub-unit-cell displacements of ions. Meanwhile, the kinetic barrier for a reduction of HfO_2 by the adjacent TiN electrode is difficult to estimate, but it should be strongly related to a diffusion of O and N ions. Thus, the kinetic barrier might be comparable to that of oxygen vacancy diffusion. The kinetic barriers of diffusion of doubly ionized and neutral oxygen vacancy are reported to be 0.5-0.7 and 2.4 eV/f.u.,[45] respectively, which is of ~1-2 orders higher than that of the t-to-o phase transition. Since a hard breakdown, which is a primary failure mechanism of the doped HfO_2, is strongly influenced by diffusion and accumulation of oxygen vacancies, low concentration of oxygen vacancies should be beneficial to achieve large electric field cycle number until breakdown. Therefore, crystallization at a lower temperature can be more effective to achieve a lower concentration of oxygen vacancies in the pristine state, although it can result in a high fraction of the non-ferroelectric t-phase. In this work, nonetheless, a rather long annealing time (4 h) during TiN electrode deposition might be useful to increase the o-phase fraction in HZLO thin films. It should be pointed out that such a strategy is possible with characteristics of HZLO distinguished from other doped HfO_2 systems. Zr is the only alloying element which decreases the crystallization temperature of HfO_2, and FE performance can be achieved with the La-concentration even lower than 1.0 mol. %, which should negligibly increase the crystallization temperature of HfO_2 thin films. As a result, the HZLO system is highly promising to achieve high endurance for future nonvolatile memory applications.

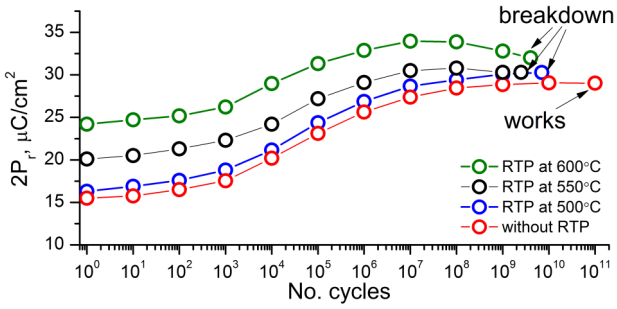

FIG. 7. Endurance characteristics measured by PUND from HZLO-based stacks with 0.7 mol. % of La without RTP and after RTP at 500, 550, and 600 °C. During PUND measurements, the pulse duration and the amplitude remained constant, 0.6 μs and 2.5 MV/cm, respectively.

CONCLUSION

In this work, a detailed analysis of the structural and electrical properties of the La-doped HfO_2-ZrO_2 films was performed according to the La-concentration in the range of 0.4-2.0 mol. %, which were compared with the undoped HfO_2-ZrO_2 film. Specifically, the crystallization of the films was not attempted by the conventional RTP at temperatures higher than 500 °C, which indeed imposed negative influence to the reliability performance, but by the thermal energy during the top TiN electrode deposition at 400 °C for 4 h by a thermal ALD. This temperature meets the BEOL-integration limitations for memory applications, without any additional high-temperature post-processing. Pure or partial ferroelectric response was demonstrated for lower La-concentrations (<≈1 mol. %), where the optimum ferroelectric performance could be achieved at the La-concentration of 0.7 mol. %. The stable pure antiferroelectric-like response due to the more preferred formation of the tetragonal phase was shown for the highest La-concentration. The most significant merit of the optimized HZLO film with the La-concentration of 0.7 mol. % was as follows. It showed an unprecedented endurance cycle up to 10^{11} without the involvement of fatigue and hard breakdown at a cycling field strength of 2.5 MV/cm. The achieved $2P_r$ after the full wake-up was as high as $\approx 28\,\mu C/cm^2$ even with the relatively low driving field strength. The degree of wake-up, i.e., the $2P_r$ ratio between the woken-up state and the pristine state was lower than half of the previous sample with similar reliability which was crystallized by RTP. Such an improvement was due to the interplay between the lowering leakage current and increasing t-phase formation tendency with the increasing La-concentration. This optimized sample also showed degraded reliability performance when it was further processed by RTP at 500-600 °C, which again demonstrates the importance of a low-temperature crystallization (at 400 °C).

SUPPLEMENTARY MATERIAL

See supplementary material for the details of the La content calculations, XPS data, SEM photographs of the La:HZO film surface, structural analysis, and results of the reproducibility test.

ACKNOWLEDGMENTS

The study of ferroelectric properties of multicomponent La:HZO films was supported by the Russian Science Foundation (Project No. 18-19-00527). The development of fully-ALD grown MIM stacks concept including ALD TiN electrodes was supported by the Ministry of Education and Science of Russian Federation (Project No. 16.9286.2017/БЧ). The authors also acknowledge MIPT Shared Facilities Center supported by the Ministry of Education and Science of Russian Federation (Grant No. RFMEFI59417X0014) for access to the equipment. The authors are also grateful to the anonymous reviewer for his helpful comments aimed to improve this work.

REFERENCES

[1]J. Mueller, T. S. Boescke, S. Mueller, E. Yurchuk, P. Polakowski, J. Paul, D. Martin, T. Schenk, K. Khullar, A. Kersch, W. Weinreich, S. Riedel, K. Seidel, A. Kumar, T. M. Arruda, S. V. Kalinin, T. Schloesser, R. Boschke, R. van Bentum, U. Schroeder, T. Mikolajick, in *IEEE International Electron Devices Meeting*, (IEEE, 2013), p. 10.8.1.
[2]J. Mueller, E. Yurchuk, T. Schloesser, J. Paul, R. Hoffmann, S. Mueller, D. Martin, S. Slesazeck, P. Polakowski, J. Sundqvist, M. Czernohorsky, K. Seidel, P. Kuecher, R. Boschke, M. Trentzsch, K. Gebauer, U. Schroeder, and T. Mikolajick, in *Symposium on VLSI Technology* (IEEE, 2012).
[3]A. Chernikova, M. Kozodaev, A. Markeev, D. Negrov, M. Spiridonov, S. Zarubin, O. Bak, P. Buragohain, H. Lu, E. Suvorova, A. Gruverman, and A. Zenkevich, ACS Appl. Mater. Interfaces **8**, 7232–7237 (2016).
[4]A. Chouprik, A. Chernikova, A. Markeev, V. Mikheev, D. Negrov, M. Spiridonov, S. Zarubin, and A. Zenkevich, Microelectron. Eng. **178**, 250–253 (2017).
[5]T. S. Boescke, J. Mueller, D. Brauhaus, U. Schroeder, and U. Boettger, Appl. Phys. Lett. **99**, 102903 (2011).
[6]S. Mueller, J. Mueller, A. Singh, S. Riedel, J. Sundqvist, U. Schroeder, and T. Mikolajick, Adv. Funct. Mater. **22**, 2412 (2012).
[7]A. G. Chernikova, D. S. Kuzmichev, D. V. Negrov, M. G. Kozodaev, S. N. Polyakov, and A. M. Markeev, Appl. Phys. Lett. **108**, 242905 (2016).
[8]U. Schroeder, C. Richter, M. H. Park, T. Schenk, M. Pesic, M. Hoffmann, F. P. G. Fengler, D. Pohl, B. Rellinghaus, C. Zhou, C.-C. Chung, J. L. Jones, and T. Mikolajick, Inorg. Chem. **57**(5), 2752–2765 (2018).
[9]M. Hoffmann, U. Schroeder, T. Schenk, T. Shimizu, H. Funakubo, O. Sakata, D. Pohl, M. Drescher, C. Adelmann, R. Materlik, A. Kersch, and T. Mikolajick, J. Appl. Phys. **118**, 072006 (2015).
[10]J. Mueller, U. Schroeder, T. S. Boescke, I. Mueller, U. Boettger, L. Wilde, J. Sundqvist, M. Lemberger, P. Kuecher, T. Mikolajick, and L. Frey, J. Appl. Phys. **110**, 114113 (2011).
[11]U. Schroeder, E. Yurchuk, J. Mueller, D. Martin, T. Schenk, P. Polakowski, C. Adelmann, M. I. Popovici, S. V. Kalinin, and T. Mikolajick, J. Appl. Phys. **53**, 08LE02 (2014).
[12]J. Mueller, T. S. Boescke, U. Schroeder, S. Mueller, D. Brauhaus, U. Boettger, L. Frey, and T. Mikolajick, Nano Lett. **12**, 4318–4323 (2012).
[13]M. H. Park, H. J. Kim, Y. J. Kim, W. Lee, T. Moon, and C. S. Hwang. Appl. Phys. Lett. **102**, 242905 (2013).
[14]M. H. Park, Y. H. Lee, H. J. Kim, T. Schenk, W. Lee, K. D. Kim, F. P. G. Fengler, T. Mikolajick, U. Schroeder, and C. S. Hwang, Nanoscale **9**, 9973–9986 (2017).
[15]A. Chouprik, S. Zakharchenko, M. Spiridonov, S. Zarubin, A. Chernikova, R. Kirtaev, P. Buragohain, A. Gruverman, A. Zenkevich, and D. Negrov, ACS Appl. Mater. Interfaces **10**(10), 8818–8826 (2018).
[16]P. Polakowski and J. Mueller, Appl. Phys. Lett. **106**, 232905 (2015).
[17]M. H. Park, H. J. Kim, Y. J. Kim, T. Moon, and C. S. Hwang, Appl. Phys. Lett. **104**, 072901 (2014).
[18]M. H. Park, H. J. Kim, Y. J. Kim, W. Lee, T. Moon, K. D. Kim, and C. S. Hwang, Appl. Phys. Lett. **105**, 072902 (2014).
[19]S. Dey, K. Tapily, S. Consiglio, R. D. Clark, C. S. Wajda, G. J. Leusink, A. R. Woll, and A. C. Diebold, J. Appl. Phys. **120**, 125304 (2016).
[20]R. Batra, T. D. Huan, G. A. Rossetti, Jr., and R. Ramprasad, Chem. Mater. **29**, 9102 (2017).
[21]M. G. Kozodaev, A. G. Chernikova, E. V. Korostylev, M. H. Park, U. Schroeder, C. S. Hwang, and A. M. Markeev, Appl. Phys. Lett. **111**, 132903 (2017).
[22]P. D. Lomenzo, Q. Takmeel, C. Zhou, C. M. Fancher, E. Lambers, N. G. Rudawski, J. L. Jones, S. Moghaddam, and T. Nishida, J. Appl. Phys. **117**, 134105 (2015).
[23]A. G. Chernikova, M. G. Kozodaev, D. V. Negrov, E. V. Korostylev, M. H. Park, U. Schroeder, C. S. Hwang, and A. M. Markeev, ACS Appl. Mater. Interfaces **10**, 2701–2708 (2018).
[24]M. H. Park, H. J. Kim, Y. J. Kim, T. Moon, K. D. Kim, and C. S. Hwang, Adv. Energy Mater. **4**, 1400610 (2014).

[25]F. Ali, X. Liu, D. Zhou, X. Yang, J. Xu, T. Schenk, J. Mueller, U. Schroeder, F. Cao, and X. Dong, J. Appl. Phys. **122**, 144105 (2017).
[26]P. D. Lomenzo, C.-C. Chung, C. Zhou, J. L. Jones, and T. Nishida. Appl. Phys. Lett. **110**, 232904 (2017).
[27]M. G. Kozodaev, Y. Y. Lebedinskii, A. G. Chernikova, S. N. Polyakov, and A. M. Markeev, Phys. Status Solidi A **214**, 1700056 (2017).
[28]D. Nečas and P. Klapetek, "Gwyddion: An open-source software for SPM data analysis," Cent. Eur. J. Phys. **10**, 181–188 (2012).
[29]S. Dey, K. Tapily, S. Consiglio, K.-H. Yu, R. D. Clark, C. S. Wajda, G. J. G. J. Leusink, A. R. Woll, and A. Diebold, MRS Adv. **04**, 269–274 (2016).
[30]M. H. Park, Y. H. Lee, H. J. Kim, Y. J. Kim, T. Moon, K. D. Kim, J. Mueller, A. Kersch, U. Schroeder, T. Mikolajick, and C. S. Hwang, Adv. Mater. **27**, 1811–1831 (2015).
[31]M. H. Park, T. Schenk, C. M. Fancher, E. D. Grimley, C. Zhou, C. Richter, J. M. LeBeau, J. L. Jones, T. Mikolajick, and U. Schroeder, J. Mater. Chem. C **5**, 4677 (2017).
[32]C. Richter, T. Schenk, M. H. Park, F. A. Tscharntke, E. D. Grimley, J. M. LeBeau, C. Zhou, C. M. Fancher, J. L. Jones, T. Mikolajick, and U. Schroeder, Adv. Electron. Mater. **3**, 1700131 (2017).
[33]M. G. Kozodaev, A. G. Chernikova, R. R. Khakimov, M. H. Park, A. M. Markeev, and C. S. Hwang, Appl. Phys. Lett. **113**, 123902 (2018).
[34]W. L. Warren, D. Dimos, B. A. Tuttle, R. D. Nasby, and G. E. Pike, Appl. Phys. Lett. **65**, 1018 (1994).
[35]S. V. Barabash, D. Pramanik, Y. Zhai, B. Magyari-Kope, and Y. Nishi, ECS Trans. **75**(32), 107–121 (2017).
[36]M. H. Park, H. J. Kim, Y. J. Kim, T. Moon, K. D. Kim, Y. H. Lee, S. D. Hyun, and C. S. Hwang, Adv. Mater. **28**(36), 7956–7961 (2016).
[37]M. Pesic, F. P. G. Fengler, L. Larcher, A. Padovani, T. Schenk, E. D. Grimley, X. Sang, J. M. LeBeau, S. Slesazeck, U. Schroeder, and T. Mikolajick, Adv. Funct. Mater. **26**(25), 4601–4612 (2016).
[38]E. D. Grimley, T. Schenk, X. Sang, M. Pesic, U. Schroeder, T. Mikolajick, and J. M. LeBeau, Adv. Electron. Mater. **2**, 1600173 (2016).
[39]M. H. Park, C. C. Chung, T. Schenk, C. Richter, K. Opsomer, C. Detavernier, C. Adelmann, J. L. Jones, T. Mikolajick, and U. Schroeder, Adv. Electron. Mater. **4**, 1800091 (2018).
[40]R. Materlik, C. Kuenneth, and A. Kersch, J. Appl. Phys. **117**, 134109 (2015).
[41]S. E. Reyes-Lillo, K. F. Garrity, and K. M. Rabe, Phys. Rev. B **90**, 140103 (2014).
[42]T. D. Huan, V. Sharma, G. A. Rossetti, and R. Ramprasad, Phys. Rev. B **90**, 064111 (2014).
[43]M. H. Park, H. J. Kim, Y. J. Kim, Y. H. Lee, T. Moon, K. D. Kim, S. D. Hyun, and C. S. Hwang, Appl. Phys. Lett. **107**, 192907 (2015).
[44]T. Schenk, M. Hoffmann, J. Ocker, M. Pesic, T. Mikolajick, and U. Schroeder, ACS Appl. Mater. Interfaces **7**, 20224–20233 (2015).
[45]N. Capron, P. Broqvist, and A. Pasquarello, Appl. Phys. Lett. **91**, 192905 (2007).